

# A Mobile and Low-Cost Spectrophotometry based Water-Quality Monitoring System using Off-the-shelf Cameras

**Nishant Sinha\***, **Ashwin Ashok\*\***

Department of Computer Science

Georgia State University

nsinha2@student.gsu.edu, aashok@gsu.edu

(\*Lead student author, \*\* faculty mentor)

## Abstract

In this paper, we design a low-cost mobile system that can use off-the-shelf web-cameras as a potential UV and visible light spectrometer by using the fundamental concepts of light sensing and computing. We qualitatively and quantitatively compare images of UV light transmitted through water containing varying contaminants and concentrations and suggest methods to train a system on learning the light transmittance parameters pertaining to the different impurities in water. In this paper, as a proof of concept, we particularly explore the tests for lead, arsenic, table salt, charcoal, and coconut oil in water.

## 1. Introduction

Spectrophotometry is a scientific technique that is used to quantitatively analyze the presence of substances, such as elements and compounds in colloids, impurities, and even dissolved substances using light. Using UV-Vis spectrophotometry, through calibration procedures, it is possible to record the wavelength range of maximum absorption of substances in a liquid medium by scanning across the range of ultraviolet and visible wavelengths ([200-850] nm) [1, 2]. From the resulting spectrograph, it is then possible to determine contaminants present in the sample [3].

Spectroscopy has previously been used to examine the quality of water bodies from satellites [4] and determine bacteria and organic compounds present in samples [5, 6]. In this work, we aim to design a water quality monitoring system that uses the fundamental scientific potential of spectrophotometry.

Traditional spectrophotometric techniques require testing (including a pre-calibration procedure) in laboratories, and spectrophotometric equipment and tools are typically bulky and costly. We take the

challenge to design a completely mobile water quality monitoring system that can run a spectrometric procedure on-site or even in real-time by developing an algorithmic model which can determine the presence of inorganic impurities in water [7, 8, 9].

### 1.1. Motivation

Water quality and sanitation is still a major concern in the United States and globally and is listed as one of seventeen the UN sustainable development goals [10]. There exist methods of testing water samples for contaminants in labs using XFR analyzers and mass-spectrometry [1, 2], however, no affordable and portable solutions exist. With water sanitation issues apparent in the US in cases like Flint, Michigan, individuals and homeowners should have access to inexpensive water-quality monitoring systems to monitor their tap water in real-time [3].

## 2. Initial Testing

UV-Vis spectrometers sample across the UV-A, UV-B, UV-C, and visible light radiation spectrums, but other techniques use infrared or only the visible light spectrum [2]. To determine the best radiation spectrum to use for our method, we analyzed the effects of water absorption across the [300-800] nm range with two light sources, measured using a commercial mobile spectrophotometer. We tested three contaminants: salt, canola oil, and flour, at varying concentrations. See appendix A for data.

### 2.1. Light-Range Spectrograph Experimentation

We found that for salt and oil in 100mL water, visible light had a more pronounced change in absorption than UV light, however, UV light was more consistent in repeat experiments than visible light. Visible light shined through the flour sample while UV light did not. Since the intensity of the UV light source was higher than the visible light source it should have also penetrated the flour and water mixture. We

narrowed this effect to two potential causes: flour settled in the sample over time or there was visible light that entered the spectrometer without going through the sample medium (ambient light or light which passed through the jar and above the surface of the sample). Infrared light had problems passing through the contaminant samples and was more difficult to detect than UV or visible light.

Through initial testing, UV light, with its consistency across experiments and its narrower frequency range, was selected for the water-quality monitoring system. From this experiment, we also considered the effects of light source intensity on the output of the monitoring system.

### 3. Spectrophotometer Experimentation

We focused on five contaminants in this study: lead [11], arsenic, table salt, charcoal, and coconut oil in water. For these contaminants, we conducted two additional sets of tests: a baseline spectrophotometry reading through a laboratory UV-Vis spectrometer, and a comparative mobile spectrophotometry reading from a commercial mobile spectrophotometer [12]. While the baseline readings serve as a ground truth to the accuracy of our method, the mobile spectrometer results provide a measure against a mobile, non-laboratory solution and served as an additional source of data.

#### 3.1. Baseline Spectrograph

Four “unknown” samples were collected from taps across Georgia. We tested these unknowns in a laboratory UV-Vis spectrometer collecting both a spectrograph from [300-800] nm and the sample’s absorbance of 5 wavelengths across the [300-400] nm range.



Figure 1. The laboratory UV-Vis spectrometer with four samples loaded.

Baseline spectrograph readings were also collected of the five contaminants—lead, arsenic, table salt, charcoal, and coconut oil—in water. Readings were taken from three concentrations against a DI water standard, from which we construct a concentration curve. See appendix B for data.

With these two datasets, we can compare the sensitivity of the proposed monitoring system and cross validate the mobile spectrometer readings.

#### 3.2. Mobile Spectrometer

The commercial mobile spectrometer we used in experimentation passes light through two spaced slits to block ambient light and allow only light entering perpendicular to the spectrometer, and uses a UV-capable webcam focused on transparent, prismatic lens held at an angle to refract light across a [300-1100] nm spectrum. Then, software generates a spectrograph based on the position and intensity values across the spectrum.



Figure 2. The webcam used in the commercial mobile spectrometer.

We captured spectrographs and images from the spectrograph’s webcam of UV light entering the four unknown samples and the five known contaminants at three concentrations. For each sample, we collect ten data points. See appendix C for data.

We captured the datapoints during the experiment outlined in 4.1. See Figure 5 for a visual of the experiment setup.

#### 4. Proposed Water-Quality Monitoring Method

Our proposed method is to use an off-the-shelf, UV-capable web-camera [13] to capture images of UV light traveling through the sample medium, and to identify the presence of contaminants in the sample based on reflectance and absorbance patterns. We specifically investigate concentrations of lead, arsenic, table salt, charcoal, and oil in water.

We first capture images of UV light entering the jar without any sample medium as a measure of the light source intensity. Then, we capture images of UV light entering 100mL DI water, and 100mL DI water with known concentrations of contaminants.

With both the proposed method datapoints and the spectrophotometer experimentation datapoints, we construct a visual concentration curve for each known contaminant. These curves can then be used to classify unknown samples based on images of UV light entering the sample.

##### 4.1. Sampling Procedure

A set of hexagonal glass jars, one for each sample, is used instead of curved glass jars to reduce reflection and distortion from UV light interactions. To each jar, 100ml of DI water is added. Each sample should be held at 23.0 Celsius [14], to which 0.5g, 1.0g, and 4.0g of contaminant—lead, arsenic, table salt, charcoal, and coconut oil—are added until dissolved or the mixture is saturated. One jar without any added contaminant is used as a control, for a total of 16 samples.



Figure 3. The hexagonal jars storing the contaminant samples in 100mL of DI water.

During experimentation, the jar should be shrouded so that no ambient light can enter. The UV-capable web-camera is positioned on top of the jar, looking down on the sample. The UV light should be positioned adjacent to the jar, such that light enters

through a flat of the jar, and so that all UV light passes through the sample medium.

Before experimenting, an image should be captured of light entering an empty jar to determine its relative intensity.



Figure 4. Determining the light intensity of the UV flashlight (right). Light enters the mobile spectrometer (left) after passing through the empty jar.

Capture ten images for each sample of the absorption and reflection of UV light using the UV-capable webcam and the commercial mobile spectrometer. For the mobile spectrometer, capture both the spectrograph and the spectrometer camera view.

Label each dataset with the capture device (UV-capable webcam or commercial mobile spectrometer) and the contaminant and concentrations: 0.5 g/dL, 1.0 g/dL, or 4.0 g/dL.



Figure 5. A side view of the experiment setup without a shroud.

#### 5. Data Analysis

To determine the viability of an algorithmic model which can identify the contaminant and its concentration based on an image using the proposed water-quality method in 4, we first qualitatively examined the results of the experiment.

Based on our qualitative analysis, we suggest quantitative patterns in our data and show the viability of an algorithmic model for determining the contaminant and its concentration from our proposed method.

### 5.1. Qualitative Data Analysis

All qualitative analysis is done in comparison to UV light entering the empty jar. Appendix D contains the datapoints used for this analysis.

At 0.5 g/dL, arsenic in water has nearly no reflectance and the light entering the medium is dimmed. At 1.0 g/dL and 4.0 g/dL, the images have no visual change from the lower concentration, which suggests that a quantitative analysis would lead to more insights in determining the concentration.

For all concentrations of charcoal tested, the UV light was unable to penetrate the medium and a fully black image was captured in the proposed method experiment. The spectrographs of the commercial mobile spectrometer support this, however a slight dip at the [300-310] nm range suggests that there might be some light penetration that can be analyzed quantitatively.

Coconut oil in water resulted in large amount of light scattering and was easy to visually determine. At 0.5 g/dL, the scattering was minimal but still visually apparent. At 1.0 g/dL the effect was more noticeable and made the contaminant visually easy to discern from the other samples. At 4.0 g/dL the effect resulted in a purple saturated image and the associated spectrograph was likewise saturated across the [300-1100] nm range.

Lead at 0.5 g/dL concentrations is visually similar to arsenic at the same concentration. At higher concentrations, however, lead creates a soft outward radial pattern of UV light entering the medium. This effect is more apparent at 1.0 g/dL than at 4.0 g/dL, likely due to the lead particles in higher concentrations absorbing more of the UV light.

Lastly, table salt in water seems to amplify the radial pattern of light entering the sample medium and dim the reflectivity of light against the jar. Oddly at 0.5 g/dL, table salt seems to absorb all UV light, but at 4.0 g/dL, it intensely reflects the UV light. There is also a color shift towards blue from the purple of the UV light, which the spectrograph reading supports. This effect is more apparent at higher concentrations. More datapoints for table salt in water is necessary to determine at what concentration the absorption to reflection shift is triggered.

### 5.2. Quantitative Analysis Insights

With sparse data, the qualitative analysis suggests that combining the datapoints from the spectrograph and the proposed method will result in more informed insights.

The image size [1280x720 pixels] of the datapoints may be computationally expensive to work with, so data reduction by summing the HSV values of the columns along each image, which would aid in reducing the computational complexity of quantitative analyses while preserving the feature set of each image.

### 5.3. Quantitative Data Analysis

Based on the HSV values of each known contaminant, presented in appendix E, there are quantitative patterns that are not visually apparent in a qualitative analysis. To generate the HSV dataset, we averaged the ten datapoints in each dataset and summed the columns along the resulting image. We then converted the RGB image to an HSV image and separated the channels.

Arsenic had unexpected variance in its HSV graph at 1.0 g/dL. Additional datapoints at a wider range of concentrations would aid in determining the cause of this variance, and to generate an algorithmic model that could account for it.

Charcoal, unsurprisingly, did have near zero HSV values at 1.0 g/dL and 4.0 g/dL concentrations. At 0.5 g/dL, however, charcoal did allow the transmittance of light, which was shown in the spectrographs but was not visually apparent in the datapoints using the proposed method. The difference in the color intensity was minimal, peaking at a value of 15, reinforcing the need for a quantitative analysis and the viability of an algorithmic model.

The HSV graphs for coconut oil did not reveal anything that was not apparent in the qualitative analysis, but the consistency between concentrations suggests that it would be ideal for initial testing with an algorithmic model.

Lead, however, had high variance between concentrations. This also suggests the need for additional concentration datapoints. The HSV graphs between 1.0 g/dL and 4.0 g/dL are more similar than between 0.5 g/dL and 1.0 g/dL, however, suggesting

data at concentrations between 0.25 g/dL and 1.0 g/dL may describe a general trend in the HSV graphs.

Table salt, unexpectedly, did show high variance in its HSV graphs between 0.5 g/dL and the higher concentrations tested. The left half of the image at 0.5 g/dL has near zero luminance, which correlates to the absorption of UV light discovered in the qualitative analysis. However, the right half of the image, as the HSV graph reveals, does indicate the presence of UV light, albeit at a value of 10. The HSV charts of the higher concentrations are similar, which may indicate that past a certain concentration threshold, the absorption and reflection of a sample changes nonlinearly with its concentration.

## 6. Conclusion

Although the qualitative analysis is not sufficient to determine both the contaminant and its concentration, as shown with 0.5 g/dL arsenic and 0.5 g/dL lead, the quantitative analysis suggests that patterns exist in the images captured which are not immediately visible.

With the quantitative analysis, data insights that are not visually apparent were discovered. Radial patterns, dimming, and scattering of light entering and exiting the sample medium seen in the qualitative analysis were similarly apparent in the HSV graph of the quantitative analysis. Quantitative analysis in conjunction with the spectrograph analysis could prove to be sufficient to train an algorithmic model on detecting the presence of a contaminant and determining its concentration in water.

## 7. Acknowledgements

Thank you to Dr. Ashwin Ashok for overseeing this research and providing insight, to Dr. Dan Deocampo for lending his UV-Vis spectrophotometer, and to Dr. Daniel Gebregiorgis for providing access to the laboratory and equipment for experiments.

## 8. References

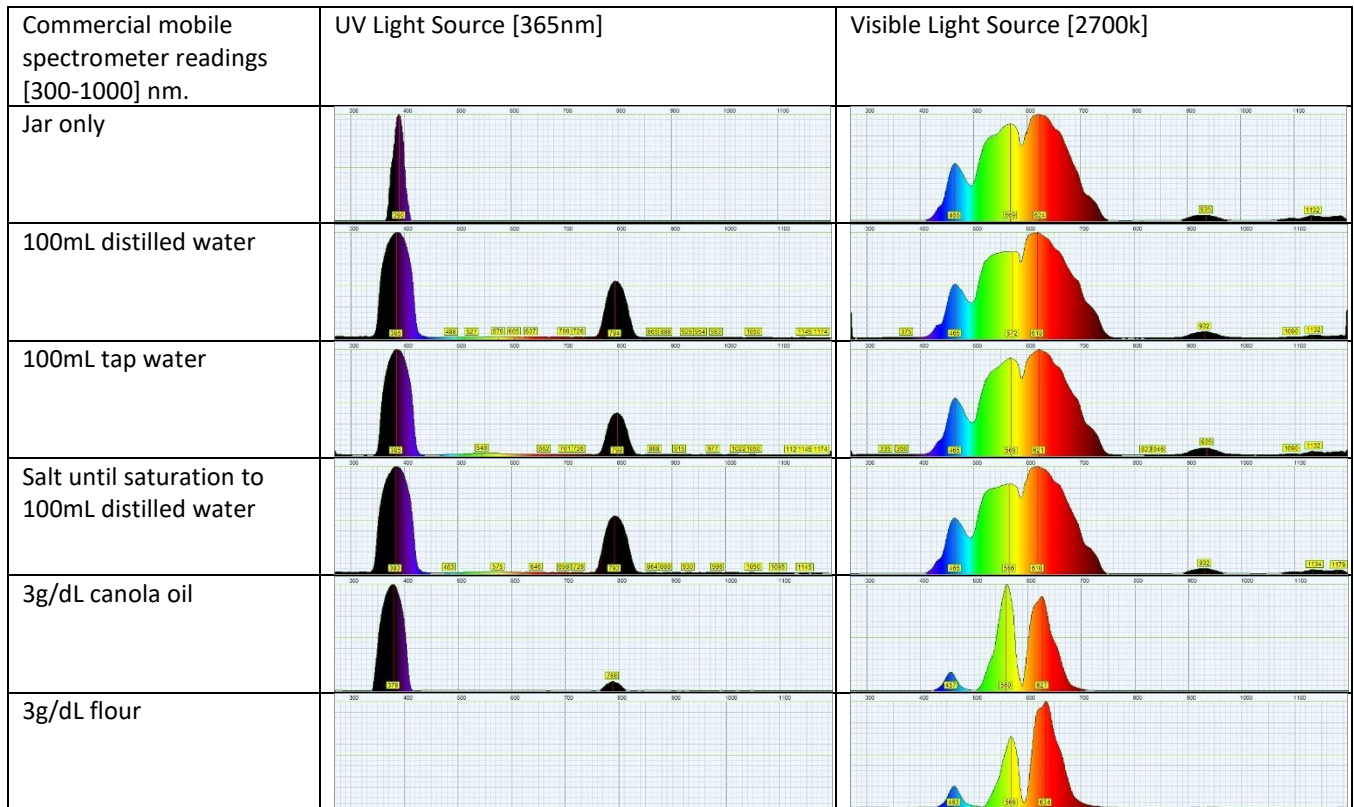
- [1] D. Harvey, "UV/Vis and IR Spectroscopy," Libretexts, Chemistry, 10.3. Updated: Jan. 5, 2017.
- [2] T. Wenzel, "Introduction to Infrared Spectroscopy," Libretexts, Chemistry, 4.1. Updated: Oct. 30, 2018.

- [3] M. Heibati, C. Stedmon, et al, "Assessment of drinking water quality at the tap using fluorescence spectroscopy," *Water Research*, vol. 125, issue 15, pp. 1-10. Nov. 15 2017.
- [4] V.E. Brando, A.G. Dekker, "Satellite hyperspectral remote sensing for estimating estuarine and coastal water quality," *IEEE Trans. Geo. Sensing*, vol. 41 issue 6, pp. 1378-1387. Jun. 2003.
- [5] J. Brodbelt, "Photodissociation mass spectrometry: New tools for characterization of biological molecules," *Chem Soc Rev.* vol 43, issue 8, pp. 2757-2783. Apr. 21, 2014.
- [6] A. Hildebrandt, R. Bragos, et al, "Performance of a portable biosensor for the analysis of organophosphorus and carbamate insecticides in water and food," *Sensors and Actuators B: Chemical*, vol. 133 issue 1, pp. 195-201. Jul. 28, 2008.
- [7] Intel AI Developer Program, "AI-Driven Test System Detects Bacteria in Water." [Online]. Available: <https://software.intel.com/en-us/articles/ai-driven-test-system-detects-bacteria-in-water>.
- [8] G.N. Siva, S. Guatam, et al, "Artificial Intelligence for Water Quality Monitoring," *J Electrochem Soc*, vol 166, issue 9. 2019.
- [9] A. Najah, A. El-Shafie, et al, "An application of different artificial intelligences techniques for water quality prediction," *International Journal of Physical Sciences*, vol 6 issue 22. Oct. 2011.
- [10] United Nation Assembly, "Sustainable Development Goals," 2015. [Online]. Available: <https://www.un.org/sustainabledevelopment/sustainable-development-goals/>.
- [11] Pharmaceutical Technology Editors, "Spectrophotometric Determination of Lead," *Pharmaceutical Technology*, vol. 32, issue 4. Apr. 02, 2008. [Online]. Available: <http://www.pharmtech.com/spectrophotometric-determination-lead>. [Accessed Mar. 01, 2019].
- [14] C. Wesley, "i-Phos Spectrometer." [Online]. Available: <http://chriswesley.org/spectrometer.htm?ref=DIYLightSpectrometerDescription5>.

[13] M. Shu, "Hack a normal camera into a UV camera." [Online]. Available: <http://mark-shu.blogspot.com/2015/08/hack-normal-camera-into-uv-camera.html>. Updated: Aug 16, 2015.



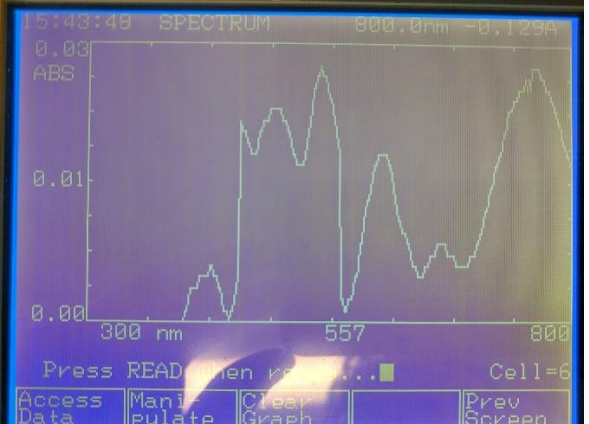
[14] Z Varkonyi, K Kabok, "Effect of temperature on light-absorption and fluorescence of the peroxidase," *Acta Biochim Biophys Acad Sci Hung*, vol. 10, issue 2, pp. 129-137. 1975.

Appendix A: initial test data.

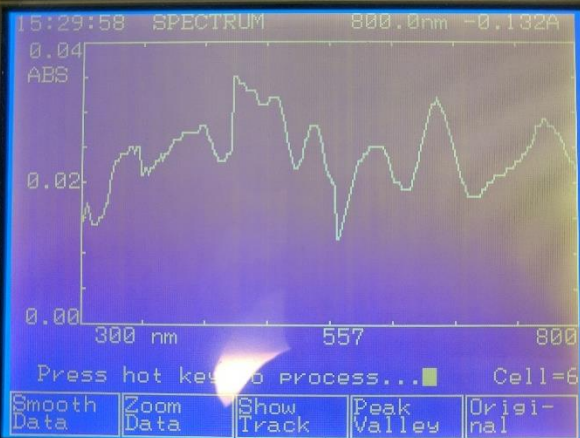
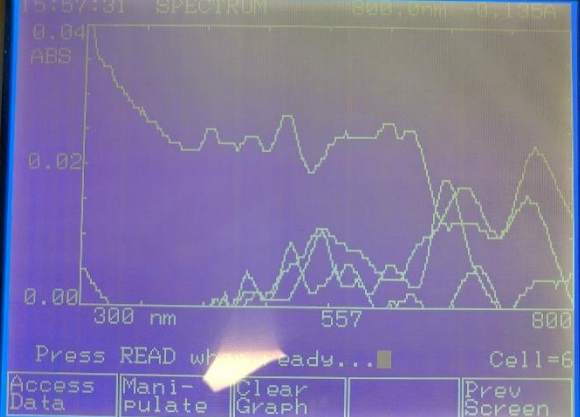




Appendix B: baseline spectrograph data.




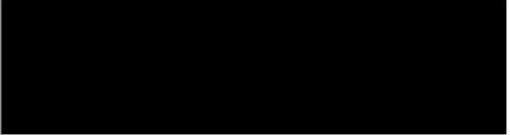


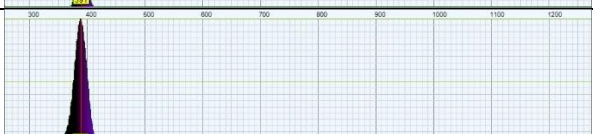
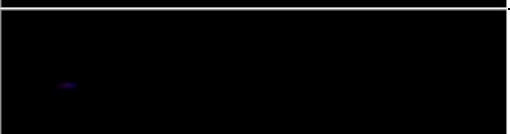


Laboratory UV-Vis spectrograph readings of unknown samples	Spectrograph	Absorption readings at $\lambda = \{300.0, 350.0, 365.0, 385.0, 400.0\}$ nm. Five tests were conducted at each wavelength.																																				
Alpharetta water source		<table><tr><th><math>\lambda</math></th><th colspan="5">Absorption (unitless)</th></tr><tr><td>300.0</td><td>.020</td><td>.001</td><td>-.025</td><td>.018</td><td>-.000</td></tr><tr><td>350.0</td><td>.015</td><td>-.009</td><td>-.026</td><td>.011</td><td>-.005</td></tr><tr><td>365.0</td><td>.018</td><td>-.009</td><td>-.020</td><td>.014</td><td>-.007</td></tr><tr><td>385.0</td><td>.017</td><td>-.011</td><td>-.020</td><td>.012</td><td>-.008</td></tr><tr><td>400.0</td><td>.016</td><td>-.011</td><td>-.019</td><td>.012</td><td>-.007</td></tr></table>	$\lambda$	Absorption (unitless)					300.0	.020	.001	-.025	.018	-.000	350.0	.015	-.009	-.026	.011	-.005	365.0	.018	-.009	-.020	.014	-.007	385.0	.017	-.011	-.020	.012	-.008	400.0	.016	-.011	-.019	.012	-.007
$\lambda$	Absorption (unitless)																																					
300.0	.020	.001	-.025	.018	-.000																																	
350.0	.015	-.009	-.026	.011	-.005																																	
365.0	.018	-.009	-.020	.014	-.007																																	
385.0	.017	-.011	-.020	.012	-.008																																	
400.0	.016	-.011	-.019	.012	-.007																																	
Athens water source		<table><tr><th><math>\lambda</math></th><th colspan="5">Absorption (unitless)</th></tr><tr><td>300.0</td><td>-.003</td><td>-.013</td><td>-.012</td><td>.017</td><td>.005</td></tr><tr><td>350.0</td><td>.003</td><td>-.009</td><td>-.008</td><td>.020</td><td>.009</td></tr><tr><td>365.0</td><td>.016</td><td>-.006</td><td>-.000</td><td>.024</td><td>.007</td></tr><tr><td>385.0</td><td>.017</td><td>-.005</td><td>.001</td><td>.025</td><td>.009</td></tr><tr><td>400.0</td><td>.017</td><td>-.004</td><td>.002</td><td>.025</td><td>.009</td></tr></table>	$\lambda$	Absorption (unitless)					300.0	-.003	-.013	-.012	.017	.005	350.0	.003	-.009	-.008	.020	.009	365.0	.016	-.006	-.000	.024	.007	385.0	.017	-.005	.001	.025	.009	400.0	.017	-.004	.002	.025	.009
$\lambda$	Absorption (unitless)																																					
300.0	-.003	-.013	-.012	.017	.005																																	
350.0	.003	-.009	-.008	.020	.009																																	
365.0	.016	-.006	-.000	.024	.007																																	
385.0	.017	-.005	.001	.025	.009																																	
400.0	.017	-.004	.002	.025	.009																																	
Downtown Atlanta water source		<table><tr><th><math>\lambda</math></th><th colspan="5">Absorption (unitless)</th></tr><tr><td>300.0</td><td>-.018</td><td>-.057</td><td>-.036</td><td>-.010</td><td>-.027</td></tr><tr><td>350.0</td><td>-.018</td><td>-.049</td><td>-.033</td><td>-.009</td><td>-.027</td></tr><tr><td>365.0</td><td>-.021</td><td>-.047</td><td>-.027</td><td>-.008</td><td>-.027</td></tr><tr><td>385.0</td><td>-.019</td><td>-.045</td><td>-.027</td><td>-.007</td><td>-.026</td></tr><tr><td>400.0</td><td>-.018</td><td>-.042</td><td>-.026</td><td>-.007</td><td>-.024</td></tr></table>	$\lambda$	Absorption (unitless)					300.0	-.018	-.057	-.036	-.010	-.027	350.0	-.018	-.049	-.033	-.009	-.027	365.0	-.021	-.047	-.027	-.008	-.027	385.0	-.019	-.045	-.027	-.007	-.026	400.0	-.018	-.042	-.026	-.007	-.024
$\lambda$	Absorption (unitless)																																					
300.0	-.018	-.057	-.036	-.010	-.027																																	
350.0	-.018	-.049	-.033	-.009	-.027																																	
365.0	-.021	-.047	-.027	-.008	-.027																																	
385.0	-.019	-.045	-.027	-.007	-.026																																	
400.0	-.018	-.042	-.026	-.007	-.024																																	














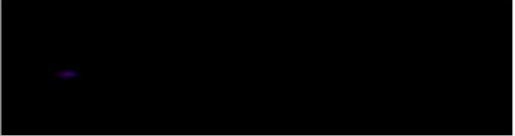








Midtown Atlanta water source		<table><tr><th><math>\lambda</math></th><th colspan="5">Absorption (unitless)</th></tr><tr><td>300.0</td><td>.023</td><td>-.026</td><td>-.026</td><td>.008</td><td>-.011</td></tr><tr><td>350.0</td><td>.034</td><td>-.010</td><td>-.012</td><td>.008</td><td>-.001</td></tr><tr><td>365.0</td><td>.038</td><td>-.005</td><td>-.002</td><td>.017</td><td>.003</td></tr><tr><td>385.0</td><td>.041</td><td>-.002</td><td>.002</td><td>.020</td><td>.006</td></tr><tr><td>400.0</td><td>.041</td><td>.000</td><td>.004</td><td>.021</td><td>.007</td></tr></table>	$\lambda$	Absorption (unitless)					300.0	.023	-.026	-.026	.008	-.011	350.0	.034	-.010	-.012	.008	-.001	365.0	.038	-.005	-.002	.017	.003	385.0	.041	-.002	.002	.020	.006	400.0	.041	.000	.004	.021	.007
$\lambda$	Absorption (unitless)																																					
300.0	.023	-.026	-.026	.008	-.011																																	
350.0	.034	-.010	-.012	.008	-.001																																	
365.0	.038	-.005	-.002	.017	.003																																	
385.0	.041	-.002	.002	.020	.006																																	
400.0	.041	.000	.004	.021	.007																																	
Combined																																						



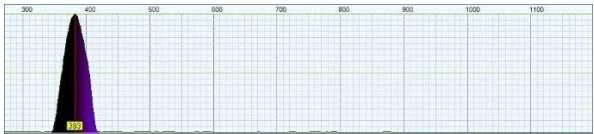

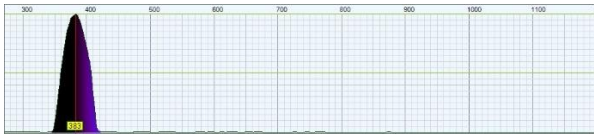
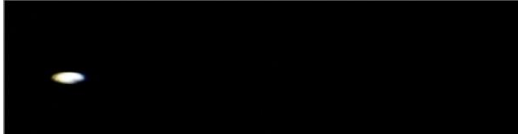






Laboratory UV-Vis readings of known samples		Absorption readings at $\lambda = 365.0$ nm. Five tests were conducted at each concentration and samples were shaken and left to settle between each reading.					
Arsenic		$\lambda$	Absorption (unitless)				
		0.5 g/dL	.061	.062	.045	.043	.055
		1.0 g/dL	.037	.096	.054	.346	.060
		4.0 g/dL	.148	.156	.183	.184	.125
Charcoal		$\lambda$	Absorption (unitless)				
		0.5 g/dL	.779	.927	.857	.794	.920
		1.0 g/dL	1.092	1.397	1.228	1.172	1.287
		4.0 g/dL	2.912	1.590	1.470	1.347	3.000
Coconut oil		$\lambda$	Absorption (unitless)				
		0.5 g/dL	.212	.210	.202	.195	.536
		1.0 g/dL	.226	.107	.105	.201	.074
		4.0 g/dL	.369	.159	.092	.131	.124
Lead		$\lambda$	Absorption (unitless)				
		0.5 g/dL	.088	.072	.251	.308	.145
		1.0 g/dL	.366	.434	.397	.410	.438
		4.0 g/dL	1.049	.718	.786	1.277	.996
Table salt		$\lambda$	Absorption (unitless)				
		0.5 g/dL	.017	.004	-.030	.005	.016
		1.0 g/dL	.032	.041	.009	.103	.055
		4.0 g/dL	.018	.000	.002	.019	.000

Appendix C: mobile spectrometer data. Contains only one of the ten images captured for each dataset.

0.5 g/dL contaminant imaged with a commercial mobile spectrometer	Spectrograph	Spectrometer camera image
Arsenic		
Charcoal		
Coconut oil		
Lead		
Table salt		


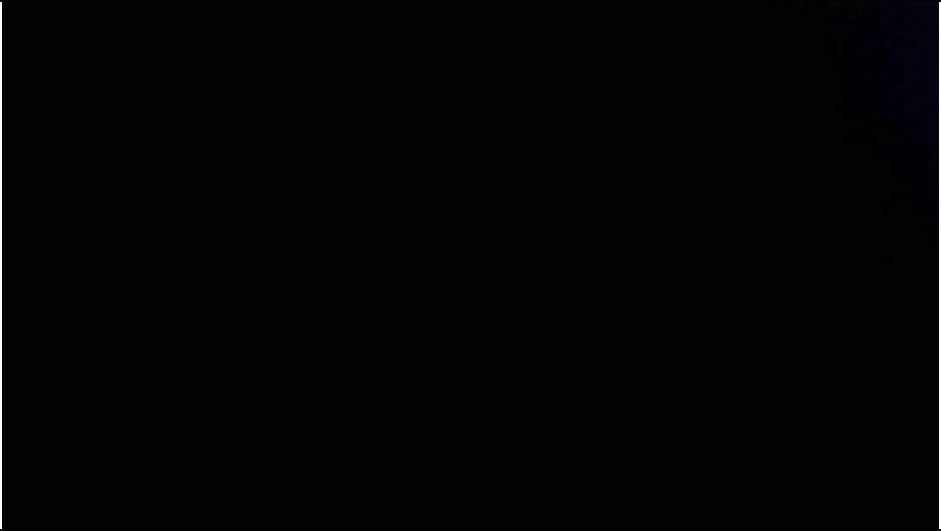
1.0 g/dL contaminant imaged with a commercial mobile spectrometer	Spectrograph	Spectrometer camera image
Arsenic		
Charcoal		
Coconut oil		
Lead		
Table salt		




4.0 g/dL contaminant imaged with a commercial mobile spectrometer	Spectrograph	Spectrometer camera image
Arsenic		
Charcoal		
Coconut oil		
Lead		
Table salt		

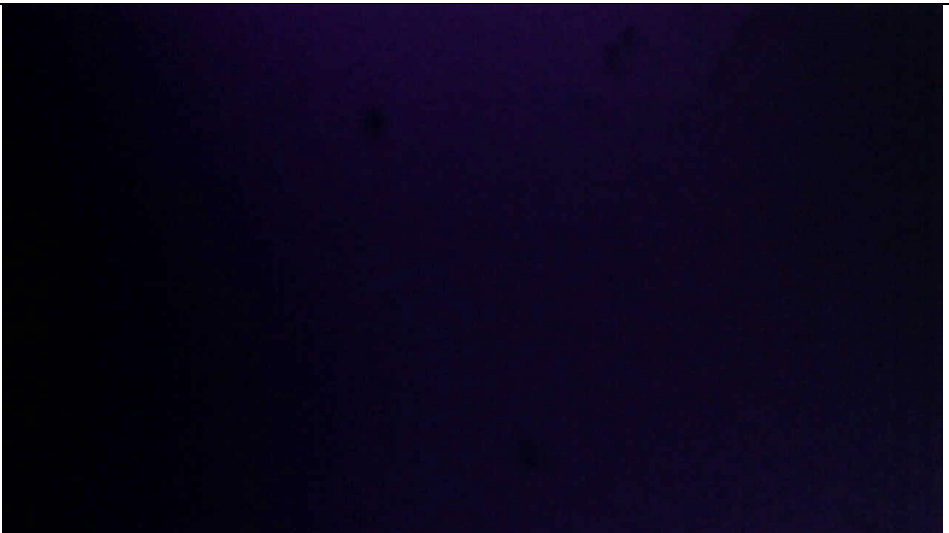
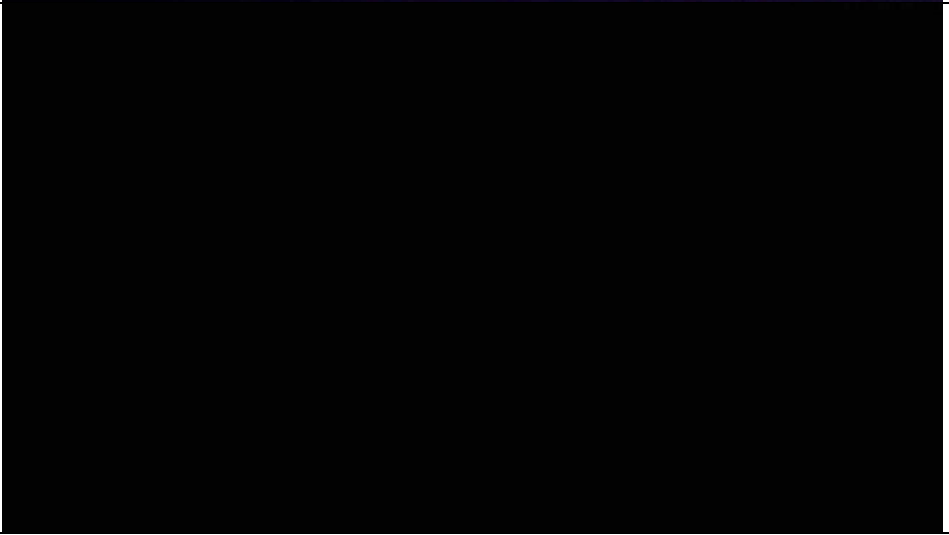
"Unknown" samples and standards imaged with a commercial mobile spectrometer	Spectrograph	Spectrometer camera image
Alpharetta, GA water sample		
Athens, GA water sample		
Downtown Atlanta, GA water sample		
Midtown Atlanta, GA water sample		
DI Water sample		
Empty jar		







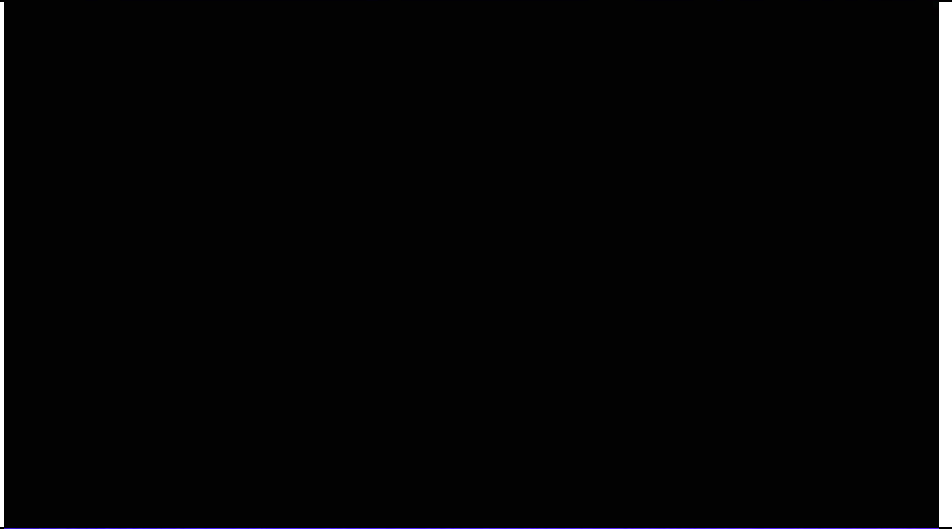

Appendix D: proposed water-quality monitoring webcam data. Contains only one of the ten images captured for each dataset.



0.5 g/dL contaminant imaged using the proposed method	Web-camera image
Arsenic	
Charcoal	

Coconut oil	
Lead	
Table salt	



1.0 g/dL contaminant imaged using the proposed method	Web-camera image
Arsenic	
Charcoal	



Coconut oil	
Lead	
Table salt	



4.0 g/dL contaminant imaged using the proposed method	Web-camera image
Arsenic	
Charcoal	
Coconut oil	

Lead	
Table salt	

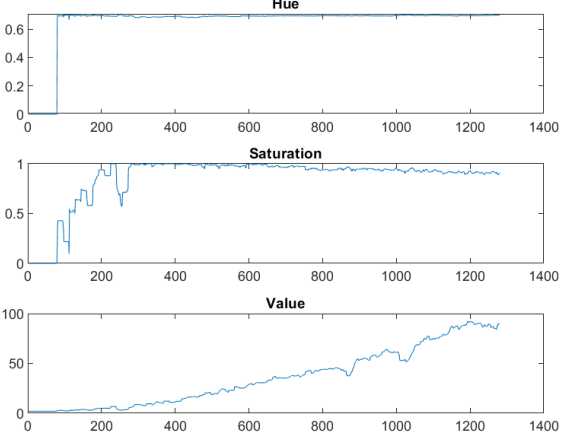
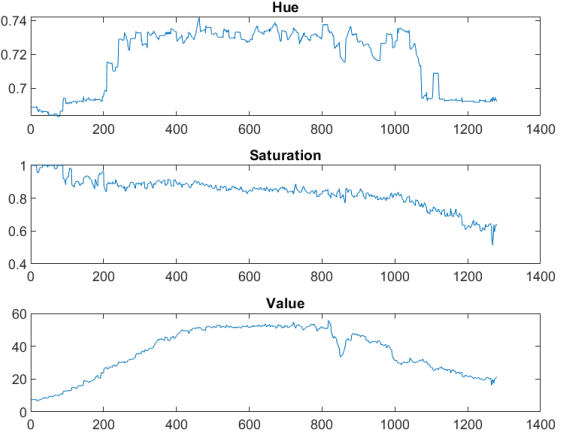
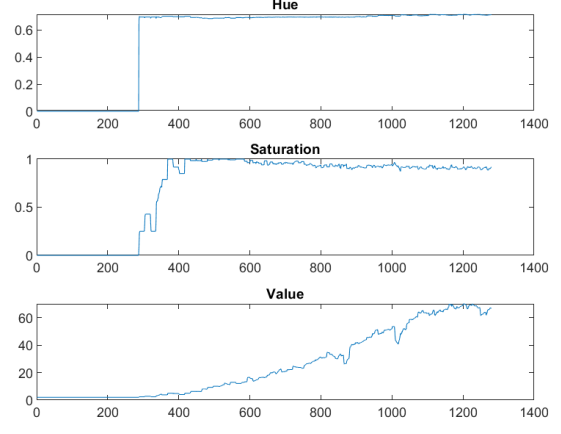


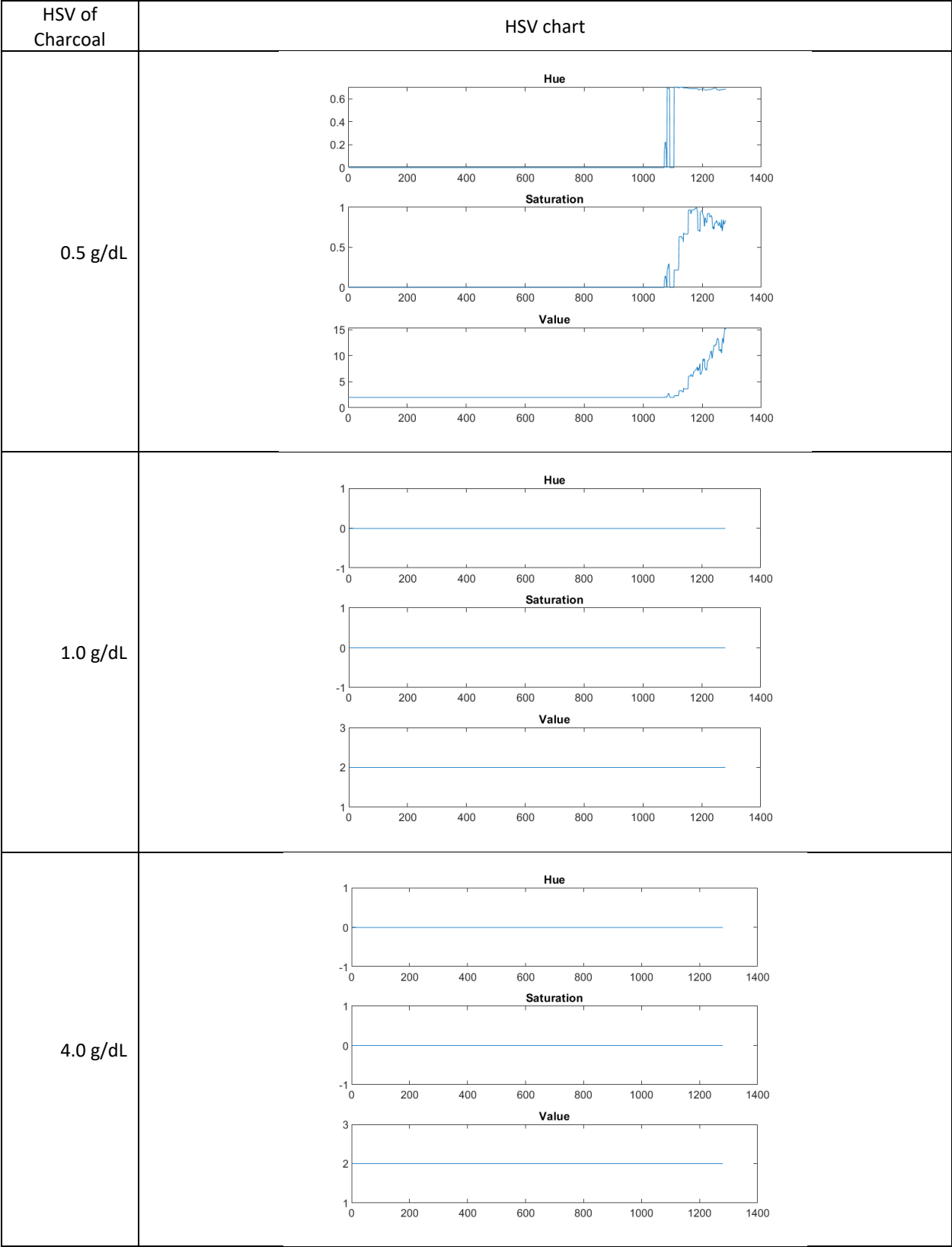
“Unknown” samples and standards imaged using the proposed method	Web-camera image
Alpharetta, GA water sample	 A dark, almost black, rectangular image with a very fine, grainy texture. There are no discernible features or patterns.
Athens, GA water sample	 A dark, almost black, rectangular image with a very fine, grainy texture. A bright, blue, diagonal streak of light is visible on the right side of the image.

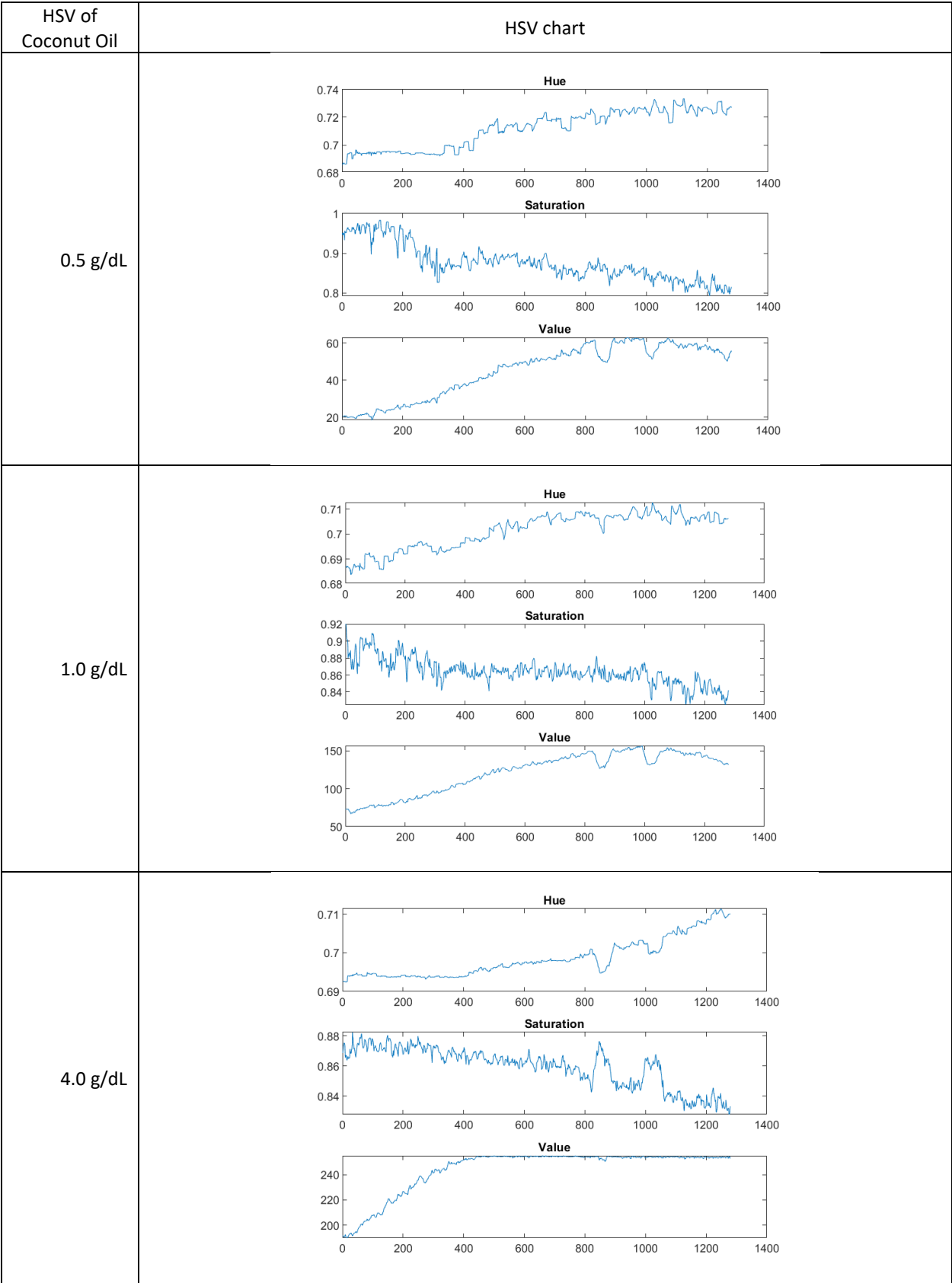
<p>Downtown Atlanta, GA water sample</p>	
<p>Midtown Atlanta, GA water sample</p>	

DI Water sample	 A fluorescence image of a DI Water sample. The image is almost entirely black, indicating a very low level of fluorescence or a very dark sample.
Empty jar	 A fluorescence image of an empty jar. The image shows a dark background with a bright, curved, yellowish-green fluorescent region on the right side, likely representing the jar's rim or a surface reflection.

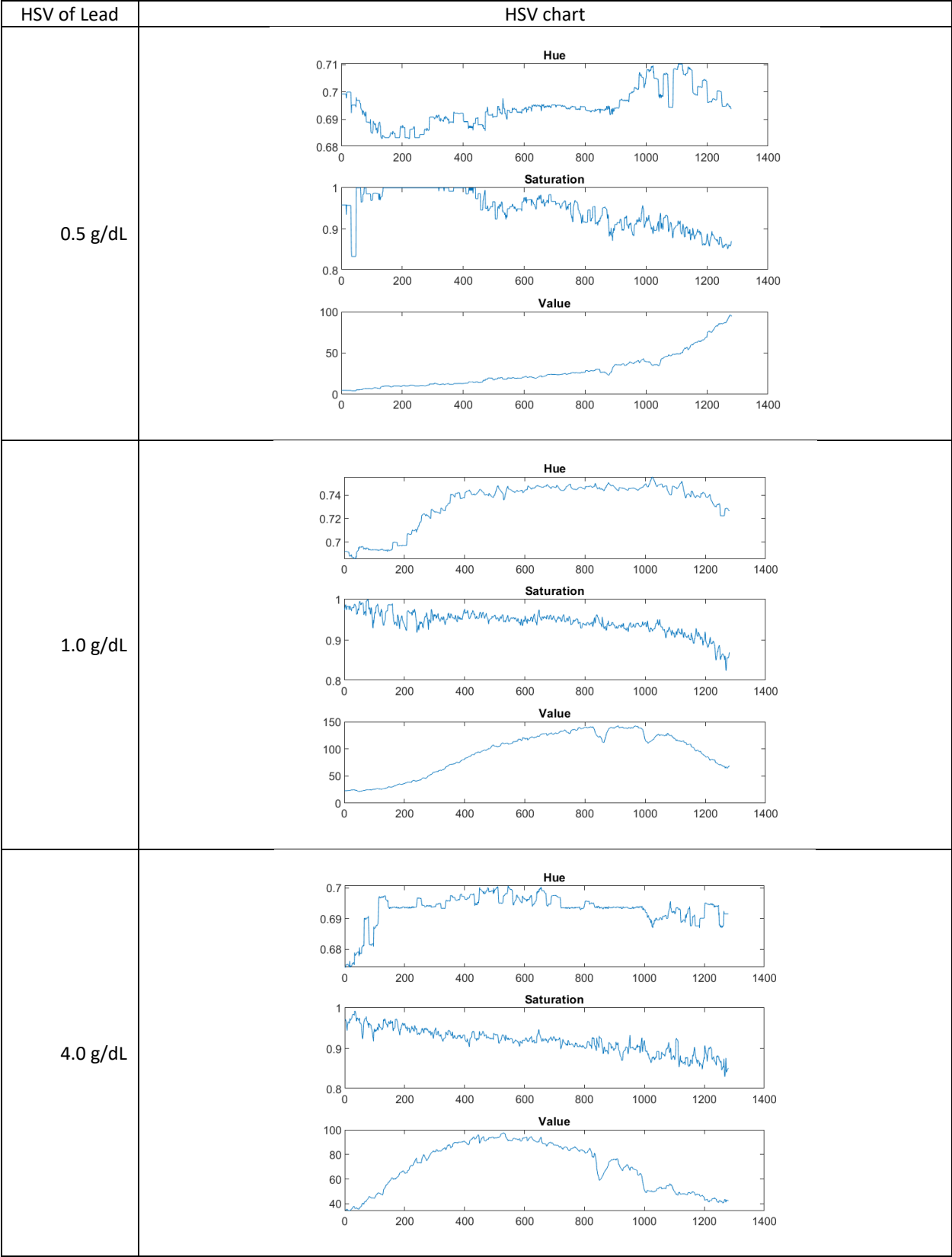
Appendix E: Quantitative data analysis. The HSV values of the mean of images captured using the proposed method. The original images are [1280x720] pixels and the horizontal axis of each chart correlates to the original image's width.

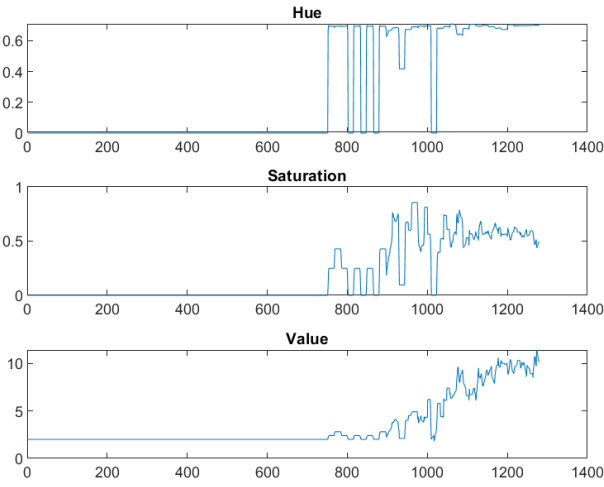
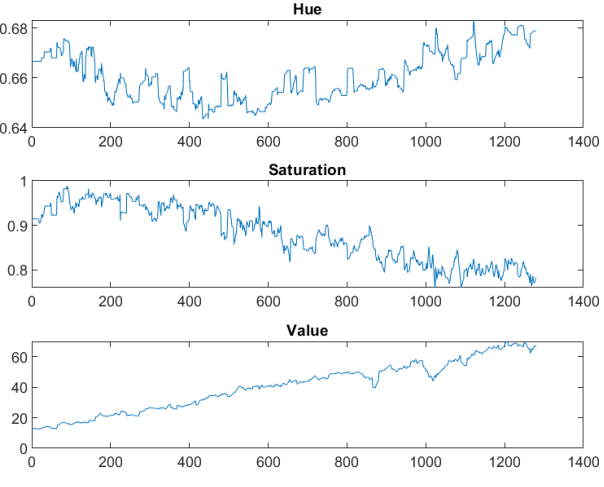
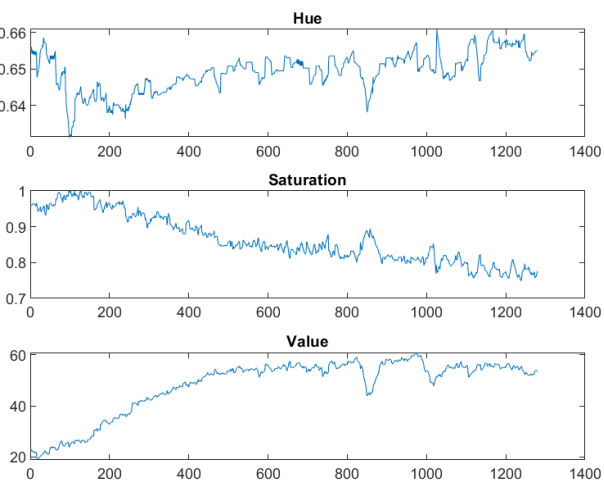
HSV of Arsenic	HSV chart
0.5 g/dL	 <p>The charts for 0.5 g/dL Arsenic show a constant Hue of approximately 0.65. Saturation starts at 0, rises to 1.0 by x=200, and remains at 1.0 until x=1300. Value starts at 0, rises steadily to about 100 at x=1300.</p>
1.0 g/dL	 <p>The charts for 1.0 g/dL Arsenic show a noisy Hue line starting at 0.7, rising to 0.74 by x=200, and remaining around 0.74 until x=1100, then dropping to 0.7. Saturation starts at 1.0, rises to 0.95 by x=200, and remains around 0.95 until x=1100, then drops to 0.6. Value starts at 0, rises to 60 by x=200, and remains around 60 until x=1100, then drops to 20.</p>
4.0 g/dL	 <p>The charts for 4.0 g/dL Arsenic show a constant Hue of approximately 0.65. Saturation starts at 0, rises to 1.0 by x=400, and remains at 1.0 until x=1300. Value starts at 0, rises steadily to about 60 at x=1300.</p>









HSV of Table Salt	HSV chart
0.5 g/dL	 <p>The charts for 0.5 g/dL show Hue values mostly between 0.6 and 0.7, Saturation values mostly between 0.5 and 1.0, and Value values mostly between 2 and 10. The Hue chart has a y-axis from 0 to 0.6. The Saturation chart has a y-axis from 0 to 1. The Value chart has a y-axis from 0 to 10. All charts have an x-axis from 0 to 1400.</p>
1.0 g/dL	 <p>The charts for 1.0 g/dL show Hue values mostly between 0.64 and 0.68, Saturation values mostly between 0.8 and 1.0, and Value values mostly between 20 and 60. The Hue chart has a y-axis from 0.64 to 0.68. The Saturation chart has a y-axis from 0.8 to 1.0. The Value chart has a y-axis from 0 to 60. All charts have an x-axis from 0 to 1400.</p>
4.0 g/dL	 <p>The charts for 4.0 g/dL show Hue values mostly between 0.64 and 0.66, Saturation values mostly between 0.7 and 1.0, and Value values mostly between 20 and 60. The Hue chart has a y-axis from 0.64 to 0.66. The Saturation chart has a y-axis from 0.7 to 1.0. The Value chart has a y-axis from 20 to 60. All charts have an x-axis from 0 to 1400.</p>